

Ocean Sequestration of Carbon Dioxide: Modeling the Deep Ocean Release of a Dense Emulsion of Liquid CO₂-in-Water Stabilized by Pulverized Limestone Particles

D. GOLOMB,* S. PENNELL, D. RYAN,
E. BARRY, AND P. SWETT

Departments of Environmental, Earth and Atmospheric Sciences, Mathematical Sciences, Chemistry, and Chemical Engineering, University of Massachusetts Lowell, Massachusetts 01854

The release into the deep ocean of an emulsion of liquid carbon dioxide-in-seawater stabilized by fine particles of pulverized limestone (CaCO_3) is modeled. The emulsion is denser than seawater, hence, it will sink deeper from the injection point, increasing the sequestration period. Also, the presence of CaCO_3 will partially buffer the carbonic acid that results when the emulsion eventually disintegrates. The distance that the plume sinks depends on the density stratification of the ocean, the amount of the released emulsion, and the entrainment factor. When released into the open ocean, a plume containing the CO₂ output of a 1000 MW_{el} coal-fired power plant will typically sink hundreds of meters below the injection point. When released from a pipe into a valley on the continental shelf, the plume will sink about twice as far because of the limited entrainment of ambient seawater when the plume flows along the valley. A practical system is described involving a static mixer for the in situ creation of the CO₂/seawater/pulverized limestone emulsion. The creation of the emulsion requires significant amounts of pulverized limestone, on the order of 0.5 tons per ton of liquid CO₂. That increases the cost of ocean sequestration by about \$13/ton of CO₂ sequestered. However, the additional cost may be compensated by the savings in transportation costs to greater depth, and because the release of an emulsion will not acidify the seawater around the release point.

Introduction

Deep ocean sequestration of the greenhouse gas CO₂ engenders strong opposition from environmental groups, marine biologists, and others because massive releases of liquid CO₂ at depth may acidify the surrounding seawater. When liquid CO₂ dissolves in seawater, carbonic acid (H₂CO₃) is formed, which may harm aquatic organisms (1). Also, it is necessary to inject the liquid CO₂ as deep as possible in order to prolong its sequestration time (2). Several methods have been proposed to mitigate the acidification problem and to make the injected CO₂ plume sink further from the release point. (a) The release of precooled liquid CO₂: Cold, liquid CO₂ is denser than seawater, making it sink deeper

from the release point while entraining ambient seawater, thus diluting the carbonic acid formed (3). (b) The release of a mixture of cold, liquid CO₂ and cold seawater: This mixture forms a solid hydrate (CO₂·6H₂O) that is negatively buoyant and hinders the dissolution of CO₂ (4,5). (c) The release of liquid CO₂ into a cylindrical open-ended vessel: This creates a dense plume that sinks further from the open bottom of the vessel while entraining ambient seawater, again diluting the carbonic acid formed (6). (d) The dispersion of liquid CO₂ droplets from a diffuser at the end of a pipe attached to a moving ship: This facilitates the dilution of the carbonic acid (7). (e) The release of a stoichiometric mixture of CO₂ and CaCO₃ in aqueous solution. The resulting solution of calcium and bicarbonate ions would not acidify the seawater around the injection point (8).

In this paper we describe the release of a dense CO₂-in-water emulsion stabilized by finely pulverized limestone particles (CaCO₃). Because the emulsion is denser than ambient seawater, the plume will sink deeper from the release point while entraining ambient seawater. Depending on the amount of emulsion released, the density stratification of the ocean, the entrainment factor, and whether the plume is released into the open ocean or on the continental slope, the plume will sink several hundred meters before it comes to density equilibrium with ambient seawater. The minimum depth of release is about 500 m; above that depth the emulsion plume would phase-separate into CO₂ gas and residual slurry of CaCO₃ in water. Laboratory experiments indicate that the emulsion is slightly alkaline, thus the plume would not acidify the surrounding seawater (9). Dissolved CaCO₃ is a natural ingredient of seawater, and a nutrient for calcareous marine organisms, such as shellfish, crustaceans, and coral. Therefore, the addition of pulverized limestone to the CO₂/seawater mix is not expected to harm marine organisms. Laboratory experiments show that to create a stable emulsion we need a weight ratio of approximately 0.5 to 1 of pulverized limestone relative to liquid CO₂, much less than the stoichiometric ratio of 2.3 to 1. While the added limestone and its pulverization increase the cost of CO₂ sequestration in the ocean, the additional cost is probably justified by the relatively benign nature of this method of CO₂ sequestration.

Liquid CO₂-Water Emulsion

Liquid CO₂ is sparingly soluble in water. Even gaseous CO₂, at atmospheric pressure and 0 °C, dissolves in water only to 0.35% by weight (10). Liquid CO₂ at 4.5 MPa and 15 °C dissolves in artificial seawater to 4.4% by weight (11). A much larger amount of liquid CO₂ can be dispersed in water by creating an emulsion stabilized by fine particles as an emulsifying agent (9, 12). The fine particles form a sheath around the dispersed CO₂ droplets, preventing their coalescence into a bulk phase. The sheathed droplets are called *globules*. The fine particles are held at the interface of the two liquids by interfacial forces. The particles act similarly to surfactants (13). The presence of fine particles enables the three-phase system, CO₂, H₂O, and fine particles, to reach an equilibrium state of minimal free energy (14). The only work that needs to be applied for the formation of the emulsion is the energy to disperse the three phases. The formation of the particle stabilized emulsion appears to be exoergic.

Tajima et al. employed a Kenics-type static mixer for the dispersion of liquid CO₂ droplets in water (15). Depending on the number of baffles in the mixer, and on the relative flow rates of liquid CO₂ and water, a narrow distribution of droplet diameters was obtained centered between 200 and

* Corresponding author phone: (978) 934-2274; fax: (978) 934-3069; e-mail: dan_golomb@uml.edu.

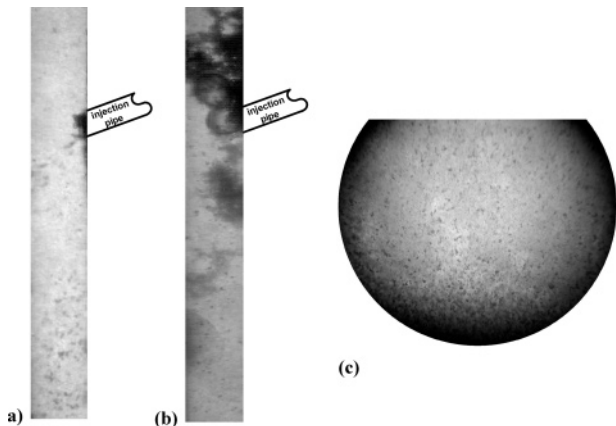


FIGURE 1. $\text{CO}_2/\text{H}_2\text{O}/\text{CaCO}_3$ emulsion in the High-Pressure Water Tunnel Facility (HWTF) and the High-Pressure Batch Reactor (HBR). (a) Side view of discharge into HWTF at 12°C , 6.8 MPa. (b) Side view of discharge into HWTF at 4°C with hydrate formation. (c) Emulsion in HBR at 12°C , 15 MPa.

$500\ \mu\text{m}$. A Kenics-type static mixer can also be employed for the creation of a $\text{CO}_2/\text{H}_2\text{O}/\text{CaCO}_3$ emulsion. Here, three fluids have to be mixed: a slurry of finely pulverized limestone in seawater, additional seawater, and liquid CO_2 . The admixing of finely pulverized limestone has the following advantages: (a) preventing the coalescence of liquid CO_2 droplets into a bulk phase; (b) creating an emulsion that is denser than ambient seawater; and (c) creating an emulsion that is slightly alkaline, not acidic (9). The mixer does not need additional mechanical power; the momentum of the feed streams is sufficient to thoroughly disperse the ingredients in the mixer and create an emulsion.

We tested the performance of a static mixer in the U.S. Department of Energy, National Energy Technology Laboratory, High-Pressure Water Tunnel Facility, HWTF. The HWTF is described in detail by Haljasmaa et al. (16). The experimental setup, test conditions and some of the results of injection of the $\text{CO}_2/\text{H}_2\text{O}/\text{CaCO}_3$ emulsion into the HWTF were described by Swett et al. (17). A $\text{CO}_2:\text{H}_2\text{O}$ flow rate of 1:10 was used. The slurry was composed of Sigma Chemicals C-4830 reagent grade CaCO_3 dispersed in reverse osmosis water. Particle size of the Sigma CaCO_3 is in the $10\text{--}15\ \mu\text{m}$ range. The outflow from the static mixer was injected into the HWTF containing 16.5 L artificial seawater kept under 6.8 MPa pressure and various temperatures. A side photo of the emulsion injection into the HWTF at 12°C is shown in Figure 1a. Individual globule diameters are in the $300\text{--}500\ \mu\text{m}$ range. A side photo of the injection at 4°C is shown in Figure 1b. Here, in addition to individual globules, CO_2 -hydrates were also formed, visible as CO_2 droplets surrounded by a hydrate film. Some of the hydrate globules appear to be positively buoyant as they move upward from the injection nozzle. It is known that CO_2 -hydrates can form in $\text{CO}_2/\text{H}_2\text{O}$ mixtures at temperatures below 10°C and pressures above 4.5 MPa (18). To avoid hydrate formation, the intake of ambient seawater to the static mixer should be from a depth where the temperature is above 10°C .

In actual deep ocean releases, it is proposed to use a $\text{CO}_2:\text{H}_2\text{O}$ ratio of 1:2, and pulverized limestone with particles in the few μm size range, which is commercially available, or it could be prepared on-site. Laboratory tests in a high-pressure batch reactor, using a $\text{CO}_2:\text{H}_2\text{O}$ ratio of 1:2, Huber Engineered Materials (Quincy, IL) Q6 pulverized limestone with a mean particle size of $2\ \mu\text{m}$ (standard deviation $1.7\ \mu\text{m}$) (12) at about 12°C and 15 MPa mixed with a magnetic stir bar at 1000 rpm, resulted in globule diameters in the $200\text{--}300\ \mu\text{m}$ range (Figure 1c). We are using a globule model consisting of an inner liquid CO_2 droplet, sheathed with a

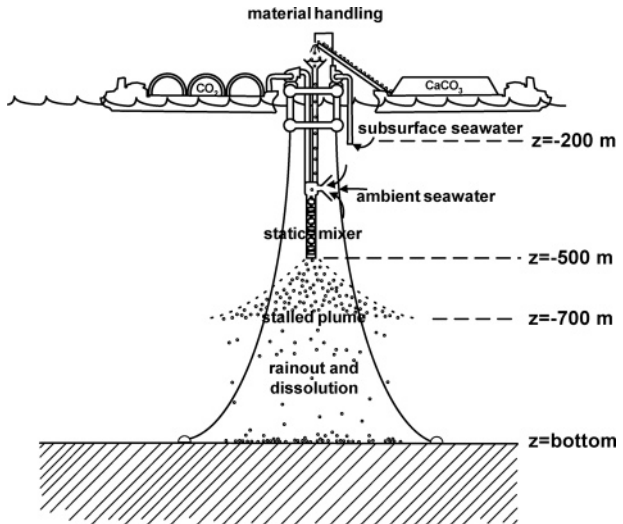


FIGURE 2. Open ocean release system.

monolayer of pulverized limestone particles (13). At 5 MPa and 10°C (typical conditions at a depth of 500 m in the ocean), the liquid CO_2 density is about $930\ \text{kg m}^{-3}$. Assuming a globule radius of $100\ \mu\text{m}$, a pulverized limestone sheath thickness of $2\ \mu\text{m}$, and pulverized limestone bulk density of $2700\ \text{kg m}^{-3}$, the CO_2 :pulverized limestone mass ratio is 1:0.2. Because we cannot be sure that all particles participate in sheathing the CO_2 droplets, and because it is desirable to have some excess CaCO_3 for buffering the carbonic acid, which may form after dissolution of the globules, we suggest using a CO_2 :pulverized limestone mass ratio 1:0.5, i.e., for every ton of liquid CO_2 , about 0.5 ton of pulverized limestone should be used. In summary, using a liquid CO_2 :seawater-volume ratio of 1:2, seawater density of $1026\ \text{kg m}^{-3}$, a liquid CO_2 :pulverized limestone mass ratio of 1:0.5, the gross density of the mixture ensuing from the static mixer is $1087\ \text{kg m}^{-3}$.

Release System

Open Ocean Release System. For injection of the emulsion into the open ocean, we visualize a system depicted in Figure 2. A floating platform is tethered to the ocean bottom. Liquid CO_2 is barged to the platform and stored in a tank. Pulverized limestone is barged to the platform and slurried with seawater pumped from a depth of about 200 m (below the photic zone). The liquid CO_2 and limestone slurry are piped to a depth of about 500 m into a static mixer. Before entering the mixer, the limestone slurry is diluted by ambient seawater, which is drawn by aspiration. As noted above, the mix ensuing from the static mixer has a gross density of $1087\ \text{kg m}^{-3}$. The only power requirements for creating the mix are for pumping seawater from a depth of 200 m into the slurry mixer, and the mechanical mixing of the slurry. No additional power is required for the undersea static mixer; the hydrostatic pressures of the liquid CO_2 and the pulverized limestone slurry provide adequate force for mixing the ingredients in the static mixer.

Off-Shore Release System. When a depth of about 500 m can be reached within 100–200 km from shore, a pipe system laid on the continental slope may be more economic than delivering the ingredients of the emulsion to a floating platform by barges. (A rigorous economic analysis of the two delivery systems is beyond the scope of this paper.) The system is depicted in Figure 3. Liquid CO_2 is stored on-shore in a tank. A slurry of pulverized limestone in seawater is prepared on-shore. The seawater for the slurry is pumped from about 200 m below the surface. Liquid CO_2 is pumped from the tank into a pipe, where it flows to a depth of about

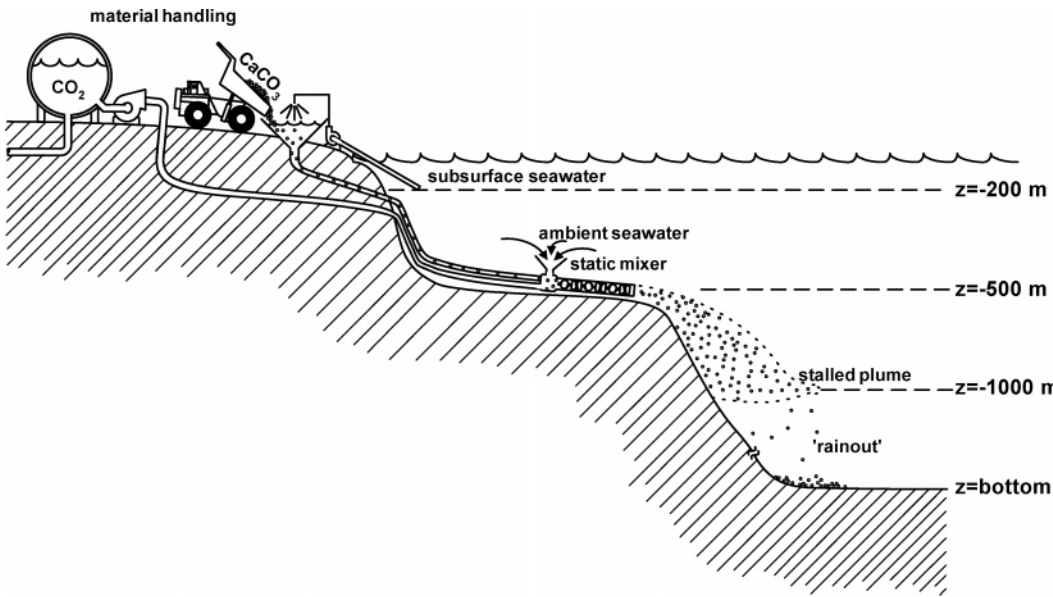


FIGURE 3. Off-shore release system.

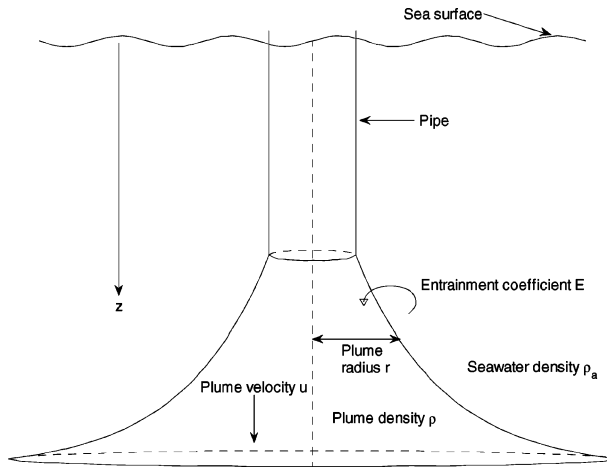


FIGURE 4. Schematic diagram of open ocean plume.

500 m, then into the static mixer. The limestone slurry is diluted with ambient seawater by aspiration before it flows into the static mixer. The mixer lies on the bottom slope. The proportion of the ingredients is the same as in the open ocean release.

Plume Modeling

Two mathematical models of plume behavior are presented in this section, one describing a vertical plume released in the open ocean and the other describing a plume released on a sloping seabed. Plume lengths are calculated for a variety of parameter values using each model. The mixture of CO_2 , limestone, and seawater emerging from the pipe is treated as a homogeneous liquid of density 1087 kg m^{-3} . It is assumed that the only effect of the globules on plume dynamics is to change the plume's density. As shown below, the Stokes' settling velocity of the globules is approximately $2 \times 10^{-3} \text{ m s}^{-1}$. This is much smaller than the plume sinking velocity, which is on the order of tenths to a few m s^{-1} .

Open Ocean Plume Model. It is assumed that the plume resulting from an open ocean emulsion release is symmetric about a vertical axis. Only steady (i.e., time-independent) plumes are considered. Three state variables are used: plume radius r , downward plume velocity u , and plume density ρ (Figure 4). All three quantities are taken to be average values over a horizontal plume cross-section, so all three depend

only on depth z . The ambient seawater is assumed to be at rest with known density profile $\rho_a(z)$. Pressure is assumed to be hydrostatic, and pressure in the plume at depth z is assumed equal to ambient pressure at the same depth. The effects of salinity and temperature variation are treated only through their combined effect on density. It is assumed that the plume entrains ambient seawater at a rate proportional to the plume velocity.

Conservation of mass, conservation of buoyancy, and the momentum equation take the following form (19)

$$\frac{d}{dz} [r^2 u] = 2Eru \quad (1)$$

$$\frac{d}{dz} [r^2 u \rho] = 2Er \rho_a \quad (2)$$

$$\frac{d}{dz} [r^2 u^2 \rho] = r^2 g(\rho - \rho_a) \quad (3)$$

Here, E denotes the entrainment coefficient (assumed constant) and g denotes gravitational acceleration. Calculations are performed using two values of E : 0.05 and 0.1. These values were chosen to bracket the value $E = 0.07$ found in ref 19. The values of the state variables are assumed known at the emulsion release depth z_0 . The model equations are solved numerically using the MATLAB routine *ode45*, an explicit, adaptive Runge–Kutta algorithm. The plume radius typically increases with depth, while plume velocity and density decrease with depth. The numerical integration is stopped when plume density reaches ambient density.

The quantity of greatest interest is the plume length, taken to be the difference between the depth at which the plume becomes neutrally buoyant and the plume release depth. As will be seen below, the ambient density profile has a significant effect on plume length. Density stratification is measured by the buoyancy frequency N , defined as

$$N^2 = \frac{g}{\rho_{as}} \frac{d\rho_a}{dz} \quad (4)$$

where ρ_{as} is the seawater density at the ocean surface. In this paper, N^2 is taken to be a constant, corresponding to linear stratification, and the ambient seawater density, ρ_{as} , at the ocean surface is taken to be 1026 kg m^{-3} . A value of 10^{-4} for N^2 corresponds to a density stratification $d\rho_a/dz$ of 1.05

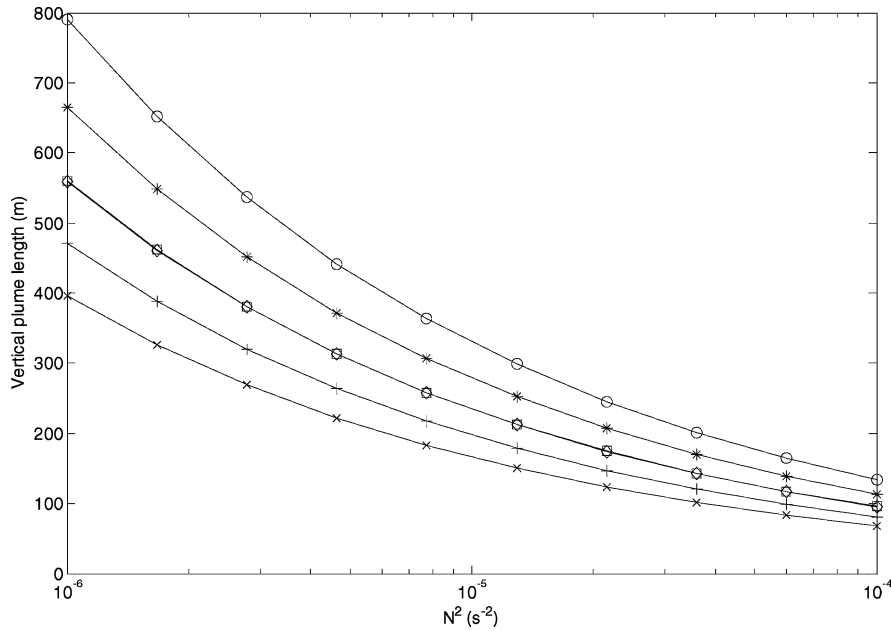


FIGURE 5. Dependence of plume length on density stratification. Circle: $E = 0.05$; CO_2 flux = 250 kg/s ($u_0 = 1.12 \text{ m/s}$). Asterisk: $E = 0.05$; CO_2 flux = 125 kg/s ($u_0 = 0.558 \text{ m/s}$). Square: $E = 0.05$; CO_2 flux = 62.5 kg/s ($u_0 = 0.279 \text{ m/s}$). Diamond: $E = 0.1$; CO_2 flux = 250 kg/s ($u_0 = 1.12 \text{ m/s}$). Plus: $E = 0.1$; CO_2 flux = 125 kg/s ($u_0 = 0.558 \text{ m/s}$). Cross: $E = 0.1$; CO_2 flux = 62.5 kg/s ($u_0 = 0.279 \text{ m/s}$). A CO_2 flux of 250 kg/s corresponds to an output of a 1000 MW_{el} coal-fired power plant. Note that the squares and diamonds overlap.

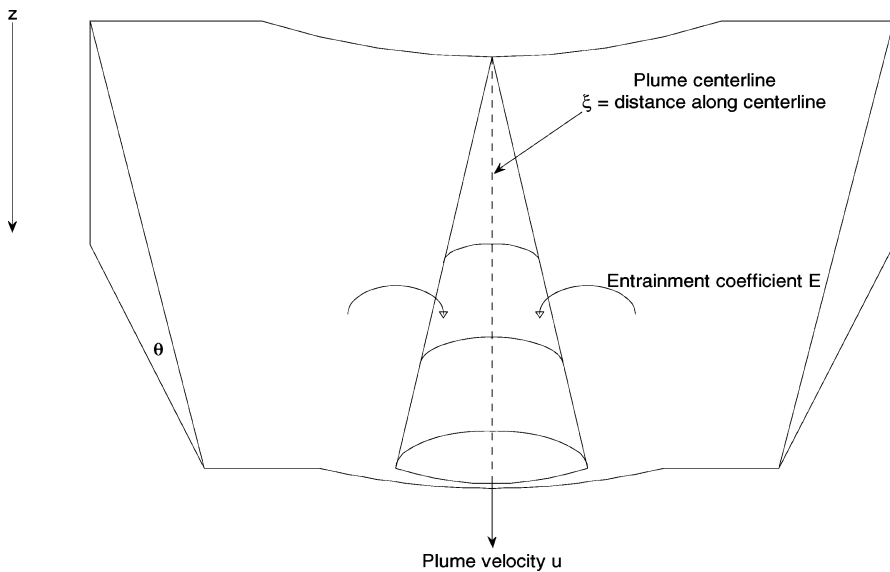


FIGURE 6. Schematic diagram of sloping seabed with valley.

$\times 10^{-2} \text{ kg m}^{-3}$ per meter, while a value of 10^{-6} for N^2 corresponds to a density stratification of $1.05 \times 10^{-4} \text{ kg m}^{-3}$ per meter.

As mentioned above, the emulsion consists of liquid CO_2 , ambient seawater, and pulverized limestone. With the volume and mass ratios of the ingredients given above, the gross density of the emulsion at the exit of the delivery pipe is 1087 kg m^{-3} . Three fluxes of liquid CO_2 are considered, 62.5, 125, and 250 kg s⁻¹, corresponding to the output of typical coal fired power plants of 250, 500, and 1000 MW electric power (20). The initial plume velocity equals the initial volume flux divided by the cross-sectional area of the delivery pipe, the radius of which is taken to be 0.5 m. For the three fluxes, the initial plume velocities are calculated as 0.279, 0.558, and 1.12 m s⁻¹, respectively.

In Figure 5 the plume length is plotted against buoyancy frequency for six sets of parameter values. In all cases, the release depth is taken to be 500 m. Note that plume length

increases as CO_2 flux increases and as stratification and entrainment coefficient decrease.

Sloping Seabed Plume Model. In the coastal release model, the plume is assumed to advance along a valley in the seabed, which is taken to be an inclined plane at angle θ with the horizontal (Figure 6). The plume is assumed to have a semicircular cross section. The independent variable is taken to be distance ξ from the release point measured along the plume bottom centerline; state variables include plume radius r , plume velocity u , plume density ρ , and depth z .

The following model equations represent conservation of mass, conservation of buoyancy, the momentum equation along the plume bottom centerline, and the geometric relationship between depth z and seabed slope θ (21).

$$\frac{d}{d\xi} [r^2 u] = Eru \quad (5)$$

$$\frac{d}{d\xi} [\rho r^2 u] = E r \rho_a \quad (6)$$

$$\frac{d}{d\xi} [\rho r^2 u^2] = g r^2 (\rho - \rho_a) \sin \theta - 2 C_D r \rho u^2 / \pi \quad (7)$$

$$\frac{dz}{d\xi} = \sin \theta \quad (8)$$

Here E denotes the entrainment coefficient and C_D denotes the coefficient of friction (assumed constant) between the plume and the seabed. The entrainment coefficient for a plume on a sloping bed is not constant but depends on the Richardson number $Ri = gr(\rho - \rho_a)\cos(\theta)/\rho u^2$ (22). The following two experimentally determined formulas for the entrainment coefficient are used (23)

$$E = \begin{cases} 0.07 & \text{for } Ri < 10^{-2} \\ 0.07Ri^{-1/2} & \text{for } 10^{-2} \leq Ri \leq 1 \\ 0.07Ri^{-3/2} & \text{for } Ri > 1 \end{cases} \quad (9)$$

and

$$E = 0.002Ri^{-1} \text{ for } 0.1 < Ri < 10 \quad (10)$$

Equation 9 is used outside the range of validity of eq 10. When both eqs 9 and 10 are valid, the average of the two values is used.

The model eqs 5–8 are solved numerically using the MATLAB routine *ode45*, with integration stopping when plume density reaches ambient density. As in the open ocean model, the quantity of greatest interest is the vertical plume length, taken to be the difference between the depth at which plume becomes neutrally buoyant and the plume release depth. Figure 6 shows the dependence of vertical plume length on density stratification for two values of the friction coefficient and three values of the CO₂ flux. In the set of curves on the left, the seabed slope is taken as 1°, while on the right the slope is taken as 10°. In all cases, the initial

TABLE 1. Effect of 10% Parameter Change on Plume Length

Open Ocean Release	
parameter	plume length change
entrainment coefficient ($E = 0.1$)	-4.6%
square of buoyancy frequency ($N^2 = 1.0 \times 10^{-5} \text{ s}^{-2}$)	-3.6%
Coastal Release	
parameter	plume length change
seabed slope (10°)	+3.8%
coefficient of friction ($C_D = 0.01$)	+1.9%

plume direction is directly downslope. Note that vertical plume length increases with decreasing stratification, with increasing seabed slope, and with increasing friction coefficient. Plumes on sloping seabeds are longer than vertical plumes in the open ocean because the entrainment rate is lower. Less plume surface area is exposed to the ambient seawater for a plume on a sloping seabed. Furthermore, friction with the seabed slows the plume velocity, further decreasing the entrainment rate (because entrainment rate is proportional to plume velocity).

Numerical experiments indicate that, for a fixed value of CO₂ flux, plume length is relatively insensitive to changes in release depth and initial plume radius. (The initial plume radius equals the radius of the pipe from which the plume flows.) Sensitivities to other parameters are shown in Table 1. For the open ocean release, the sensitivities are shown in the upper part of the table; for the slope release, the sensitivities are shown in the lower part of the table. To generate the tabulated values, each of the parameters, in turn, is increased by 10% with the others held fixed at the listed values, and the resulting change in plume length is calculated. For the open ocean release the greatest sensitivity to plume length is the entrainment coefficient, followed by the buoyancy frequency. For the slope release, in addition

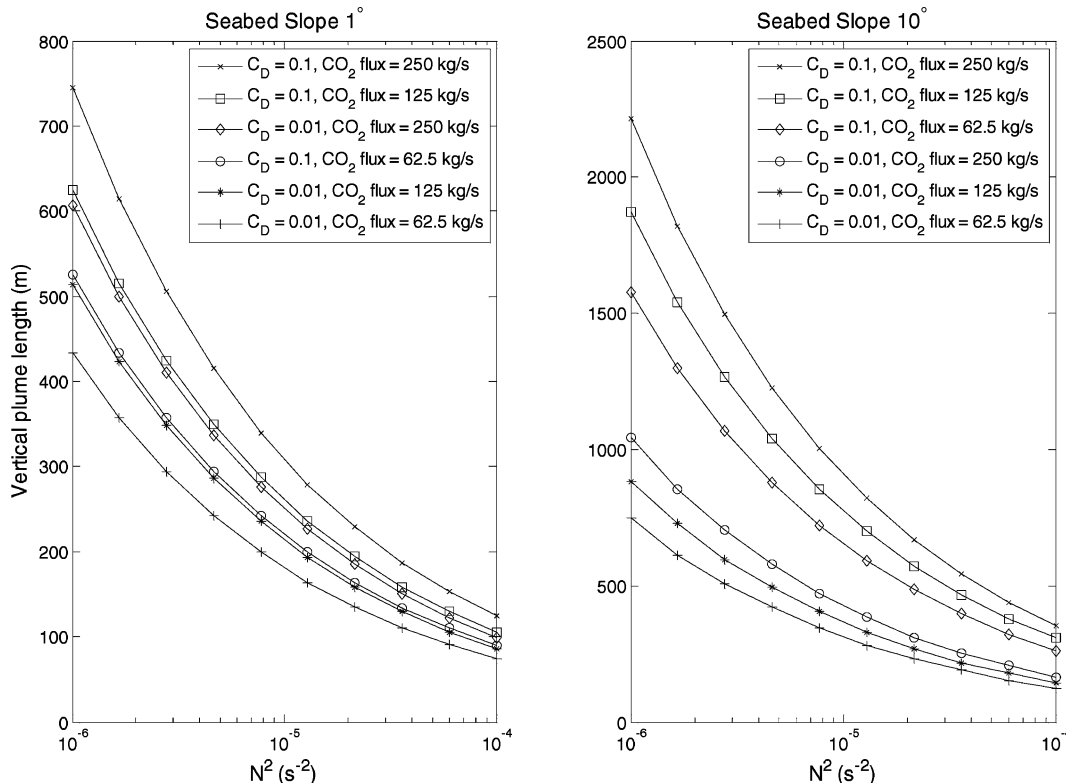
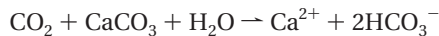


FIGURE 7. Vertical plume length vs density stratification for seabed with slope 1° (left) and 10° (right).

to the entrainment coefficient and buoyancy frequency, the seabed slope and the coefficient of friction affect the plume length. Sensitivities for the slope release case are comparable to those calculated by Adams et al. (24) for a solution of CO₂ dissolved in seawater.

Ultimate Fate of Globules

The above modeling studies show that the dense plume comes to rest when sufficient ambient seawater is entrained, so that its density asymptotically reaches the density of the ambient seawater. The question of what happens to the globules, i.e., the ultimate fate of the liquid CO₂ droplets that are sheathed with fine limestone particles is of primary concern. Laboratory experiments showed that the globules are stable during observational periods of several hours (9). The experiments also showed that the globules are heavier than ambient water, for they settled in the bottom of the water-filled high pressure observation cell. Therefore, we postulate that after the plume comes to rest, the globules, together with excess pulverized limestone, will "rain-out" from the plume on their way to the ocean bottom. Using Stokes' law for the settling of small particles in a viscous medium, we estimate that 100 μm radius globules sheathed with a 2 μm thick layer of limestone particles sink at a velocity of approximately 2×10^{-3} m s⁻¹, that is, about 200 m d⁻¹. Because the limestone particles are held by interfacial forces between the dispersed liquid CO₂ droplets and external seawater, it is unlikely that the sheath will rapidly dissolve during the fall to the ocean bottom. Eventually, the globules may disintegrate due to wave action and bottom friction. A part of the dissolved carbonic acid may be buffered by the CaCO₃ particles, according to the following reaction:



The mix ensuing from the static mixer contains 0.5 g CaCO₃ per g of CO₂ compared to a stoichiometric ratio of 2.3 g CaCO₃ per g of CO₂, not sufficient to completely buffer the carbonic acid. The rest of the dissolved carbonic acid may be dispersed and diluted over the ocean bottom. Further studies are warranted on the sensitivity of benthic organisms to diluted carbonic acid.

Economics

Huber Engineered Materials, Quincy, IL, sells pulverized limestone Q6 for \$38/t FOB. It has a mean particle size of 2 μm and a composition of 96.5% CaCO₃, 2% MgCO₃, 1% silica and silicates and 0.5% others. Alternatively, raw limestone in chunks can be purchased from several quarries for \$5–10/t FOB, and milled to the desired size on-site. In this case the major cost elements are the capital and operating costs of the grinding mills, resulting in a total cost of about \$13 per ton of pulverized limestone, including the cost of raw material and shipping. Because we need approximately 0.5 ton of pulverized limestone per ton of liquid CO₂, the total cost of providing the pulverized limestone on site is about \$6.5 per ton of liquid CO₂, not including the capital and operating cost of the slurry mixer, which may double the cost of preparing the slurry. Currently, the cost estimates of capturing and liquefying CO₂ at a coal-fired power plant range from \$15 to \$75/t CO₂ (25). Thus, the sequestration of liquid CO₂ in the form of an emulsion would add about 20% to 90% to the capture cost of CO₂, excluding transport costs to the injection site. However, this additional cost may be justified on account of increasing the sequestration period of the released CO₂, and of not acidifying the seawater around the injection point.

In conclusion, a system is described that can deliver an emulsion of liquid CO₂ in seawater stabilized by finely

pulverized limestone. Because the emulsion is denser than seawater, the injected plume will sink deeper from the release point. Depending on the flux of the emulsion and ocean density stratification, the emulsion plume will sink several hundred meters below the injection point when released into the open ocean. When released along a sloping ocean bed, the plume will sink about twice as much. Because the emulsion consists of limestone particle sheathed CO₂ droplets, the CO₂ may not dissolve immediately in seawater, thus preventing the acidification of seawater around the injection point.

Acknowledgments

This work was supported by a cooperative agreement with the U.S. Department of Energy, National Energy Technology Laboratory, no. DE-FC26-02NT41441. However, neither the U.S. Government, nor any agency thereof, nor any of their employees, makes any warranty, expressed or implied, or assumes any legal liability or responsibility for the accuracy, completeness, or usefulness of any information, apparatus, product, or process disclosed in this paper. The views and opinions of authors expressed herein do not necessarily state or reflect those of the U.S. Government or any agency thereof. We are grateful to Dr. Heino Beckert, DOE/NETL, for guidance and valuable comments throughout this cooperative agreement. We are also grateful to Robert Warzinski and Ronald Lynn of DOE/NETL for setting up and assisting in the High-Pressure Water Tunnel Facility tests, and to Michael Woods for technical help in executing the laboratory experiments. Jonathan Hedge performed the economic and energy analysis of pulverizing limestone. We are grateful to the reviewers for their helpful comments.

Literature Cited

- (1) Seibel, B.; Walsh, P. J. Potential impacts of CO₂ injection on deep-sea biota. *Science* **2001**, *294*, 319–320.
- (2) Wilson, T. R. S. The deep ocean disposal of carbon dioxide. *Energy Convers Manage*. **1992**, *33*, 627–633.
- (3) Aya, I.; Yamane, K.; Shiozaki, K. Proposal of Self-Sinking CO₂ Sending System: COSMOS. In *Greenhouse Gas Control Technologies*; Elsevier: New York, 1999; pp 269–274.
- (4) Brewer, P. G.; Friederich, G.; Peltzer, E. T.; Orr, F. M., Jr. Direct experiments on the ocean disposal of fossil fuel CO₂. *Science* **1999**, *284*, 943–945.
- (5) Riestenberg, D.; Tsouris, C.; Brewer, P. G.; Peltzer, E.; Walz, P.; Chow, A.; Adams, E. E. Field studies on the formation of sinking CO₂ particles for ocean sequestration: Effects of injector geometry on particle density and dissolution rate and model simulation of plume behavior. *Environ. Sci. Technol.* **2005**, *39*, 7287–7293.
- (6) Adams, E. E.; Golomb, D.; Zhang, X. Y.; Herzog, H. J. Confined release of CO₂ into Shallow Seawater. In *Direct Ocean Disposal of Carbon Dioxide*; Terra Scientific Publishing Company: Dordrecht, 1995; pp 153–164.
- (7) Nakashiki, N.; Ohsumi, T.; Katano, N. Technical view of CO₂ transportation onto the deep ocean floor and dispersion at intermediate depths; Terra Scientific Publishing Company: Dordrecht, 1995; pp 183–193.
- (8) Caldeira, K.; Rau, K. H. Accelerating carbonate dissolution to sequester carbon dioxide in the ocean: Geochemical implications. *Geophys. Res. Lett.* **2000**, *27*, 225–228.
- (9) Golomb, D.; Barry, E.; Ryan, D.; Lawton, C.; Swett, P. Limestone particle stabilized macro-emulsion of liquid and supercritical carbon dioxide in water for ocean sequestration. *Environ. Sci. Technol.* **2004**, *38*, 4445–4450.
- (10) CRC Handbook of Chemistry and Physics; CRC Press: Boca Raton, FL, 2000.
- (11) Munjal, P.; Stewart, P. B. Correlation equation for solubility of carbon dioxide in water, seawater, and seawater concentrates. *J. Chem. Eng. Data*. **1971**, *16*, 170–172.
- (12) Golomb, D.; Barry, E.; Ryan, D.; Swett, P.; Duan, H. Macro-emulsions of liquid and supercritical CO₂-in-water and water-in-liquid CO₂ stabilized by fine particles. *Ind. Eng. Chem. Res.* **2006**, *45*, 2728–2733.
- (13) Shaw, D. J. *Introduction to Colloid and Surface Chemistry*, 4th ed; Butterworth-Heinemann: Oxford, 1992, pp 266–269.

- (14) Kralchevsky, P.; Ivanov, A. I. B.; Ananthapadmanabhan, K. P.; Lips, A. On the thermodynamics of particle stabilized emulsions: Curvature effects and catastrophic inversion. *Langmuir* **2005**, *21*, 50–63.
- (15) Tajima, H.; Yamasaki, A.; Kiyono, F.; Teng, H. Size distribution of CO₂ drops in a static mixer for ocean disposal, *Am. Inst. Chem. Eng. J.* **2006**, *52*, 2991–2996.
- (16) Haljasmaa, I. V.; Vipperman, J. S.; Lynn, R. J.; Warzinski, R. P. Control of a fluid particle under simulated deep-ocean conditions in a high-pressure water tunnel, *Rev. Sci. Instrum.* **2005**, *76*, 025111.
- (17) Swett, P.; Golomb, D.; Ryan, D.; Barry, E.; Pennell, S.; Warzinski, R.; Lynn, R. Testing and Evaluation of a Static Mixer for Creation of a CO₂-in-Water Emulsion Stabilized by Pulverized Limestone. In *Proceedings of the 8th International Conference on Greenhouse Gas Control Technologies*; Elsevier: New York, 2006; available as CD.
- (18) Song, K. Y.; Kobayashi, R. Water content of CO₂ in equilibrium with liquid water and/or hydrates, *SPE Form. Eval.* **1987**, *500*.
- (19) Crounse, B. C.; Sokolofsky, S. A.; Adams, E. E. Bubble and Droplet Plumes in Stratification 2: Numerical Studies. In *Proceedings of the 5th International Symposium on Stratified Flows 2000*; Lawrence, G. A., Pieters, R., Yonemitsu, N., Eds.; Vancouver, BC, 2000.
- (20) Herzog, H.; Golomb, D.; Zemba, S. Feasibility, modeling and economics of sequestering power plant CO₂ emissions in the deep ocean. *Environ. Progress* **1991**, *10*, 64–74.
- (21) Alendal, G.; Drange, H.; Haugan, P. M. Modelling of Deep-Sea Gravity Currents Using an Integrated Plume Model. In *The Polar Oceans and Their Role in Shaping the Global Environment*; Johannessen, O. M., Muench, R. D., Overland, J. E., Eds.; American Geophysical Union: Washington, DC 1994; pp 237–246.
- (22) Turner, J. S. *Buoyancy Effects in Fluids*; Cambridge University Press: Cambridge, 1973; p 159.
- (23) Christodoulou, G. C. Interfacial mixing in stratified flows. *J. Hydraul. Res.* **1986**, *24*, 77–92.
- (24) Adams, E. E.; Caulfield, J. A.; Zhang, X.-Y. Sinking of a CO₂-Enriched Ocean Gravity Current. In *Proceedings of the 27th IAHR Congress*, San Francisco, August 1997, pp 352–357.
- (25) Intergovernmental Panel on Climate Change (IPCC): *Special Report on Carbon Dioxide Capture and Storage*; IPCC: Geneva, Switzerland, 2005.

Received for review September 7, 2006. Revised manuscript received April 19, 2007. Accepted April 25, 2007.

ES062137G